ACS APPLIED POLYMER MATERIALS

pubs.acs.org/acsapm Article

pH-Sensitive Degradable Coatings Releasing Antibacterial Phosphonium Species and Gentamicin

Mónica Vásquez Peña, Paul J. Ragogna, and Elizabeth R. Gillies*

Cite This: ACS Appl. Polym. Mater. 2024, 6, 12237−12246 Read Online

ACCESS | Metrics & More | Article Recommendations | Supporting Information

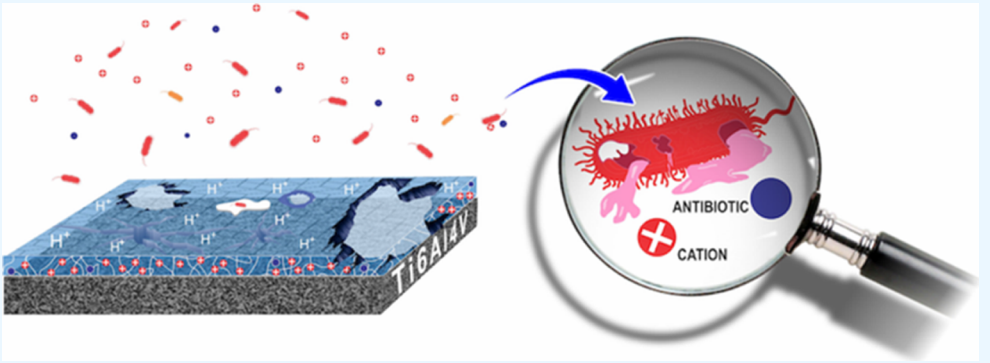

ABSTRACT: Bacterial biofilms are a growing challenge across multiple fields but particularly for biomedical devices where treatment with conventional systemic antibiotics is challenging. Approaches that lead to the killing or inhibition of bacterial growth on surfaces are gaining increasing attention. We recently reported phosphonium polymer surfaces, containing pH-sensitive acetal cross-linkers, that killed bacteria more effectively at the mildly acidic pH values associated with bacterial infection. Here, we describe the addition of the antibiotic gentamicin (GM) into the coating formulations with the aim of enhancing the antibacterial activity of the coatings. GM was functionalized with a polymerizable styrenic group via a pH-sensitive imine linkage and this monomer was successfully incorporated into cured films containing tributyl(4-vinylbenzyl)phosphonium chloride (BuP) or triphenyl(4-vinylbenzyl)phosphonium chloride (PhP) monomers and ketal (XK) or acetal (XA) cross-linkers. After incubation at pH 5, coatings composed of PhP, XK, and GM released the highest-activity antibacterial products against *Staphylococcus aureus* (*S. aureus*) compared to the other coatings. However, all PhP coatings completely inhibited the growth of *S. aureus* on their surfaces and BuP coatings led to about a 4-log reduction in bacterial colony-forming units, indicating effective contact killing. Fluorescence microscopy imaging revealed only trace levels of bacteria on the surfaces, even following incubation with 10^7 CFU/mL *S. aureus*.

KEYWORDS: *antibacterial, phosphonium, coating, acetal, pH-sensitive, gentamicin, surface*

INTRODUCTION

Biofilms are a growing challenge across various fields ranging from food processing[1] to biomedical devices.[2] In particular, infection has become a major complication associated with orthopedic devices such as screws, nails, and plates used in trauma surgeries, as well as knee and hip replacements used in joint arthroplasties.[3,4] Biofilms are particularly challenging to treat as the bacteria growing in biofilms are regularly resistant to antibiotics and are protected from the host's immune system.[5,6] Treatment of orthopedic device-related infection frequently requires one or more revision surgeries accompanied by high doses of local and/or systemic antibiotics, resulting in prolonged hospitalization, high cost, delayed recovery, and a significant risk of reinfection.[3,4] Therefore, there is significant interest in approaches that can prevent or less invasively treat such infections.

Clinically, most approaches to treating biofilm-related infections have relied on antibiotics. While systemic antibiotic therapy often accompanies revision surgeries to treat infection, it is generally not highly effective due to the poor biofilm penetration of antibiotics.[7,8] To achieve more localized release, antibiotics such as gentamicin (GM), are often loaded into poly(methyl methacrylate) (PMMA) bone cement spacers as part of a multistep revision surgery protocol.[9,10] However, as PMMA is not biodegradable, a large fraction of the antibiotic remains unreleased and therapeutic levels are only released in the first few hours postsurgery.[11−13] Resorbable antibiotic reservoirs such as calcium phosphate have also been explored,

Received: July 28, 2024
Revised: September 10, 2024
Accepted: September 17, 2024
Published: September 24, 2024

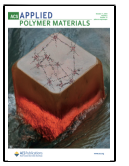

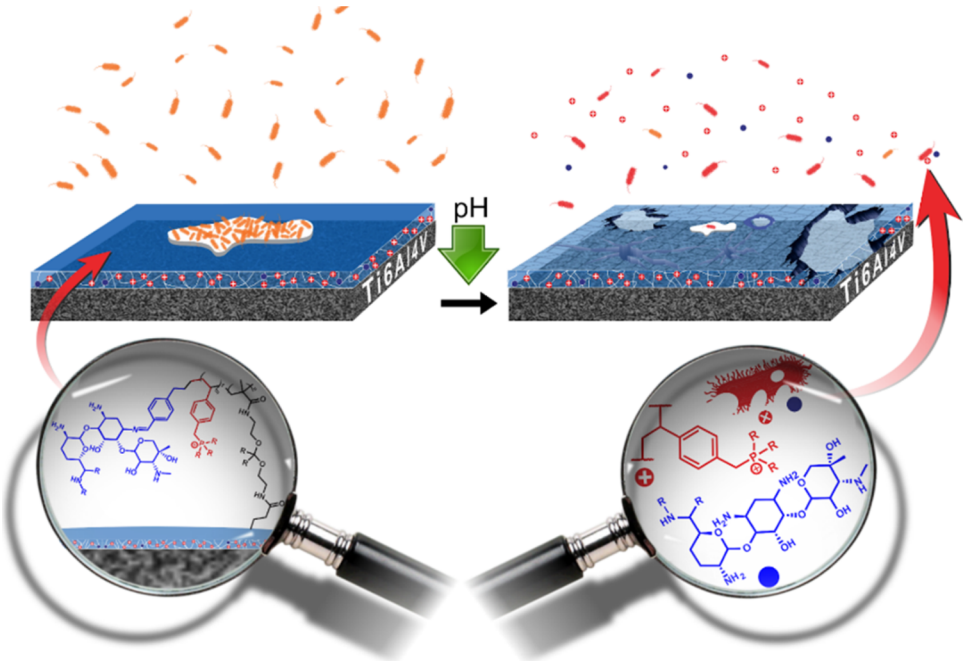

Figure 1. pH-sensitive GM-containing phosphonium coatings break down under mildly acidic conditions, releasing phosphonium molecules, gentamicin, and bacteria.

but tend to exhibit a large initial burst release of antibiotic.[14−17] Alternatively, the covalent attachment of antibiotics to the implant surface has been proposed. For example, daptomycin[18] and vancomycin[19] have been conjugated to titanium alloy surfaces by oligo(ethylene glycol) spacers, resulting in reduced colonization by *Staphylococcus aureus* (*S. aureus*) compared to control surfaces.

Approaches have also been explored to inhibit biofilm formation on surfaces. For example, antibacterial agents such as silver[20] or nitric oxide[21] have been incorporated into coatings for controlled release. Surfaces having cationic ammonium, phosphonium, or sulfonium groups have been demonstrated to kill bacteria by mechanisms involving the disruption of their anionic cell membranes.[22−25] On the other hand, antifouling coatings based on zwitterionic polymers[26] or poly(ethylene glycol) (PEG)[27,28] are aimed at preventing the initial attachment of bacteria to surfaces.

There is also growing interest in the development of stimuli-responsive antibacterial surfaces.[29−31] Such surfaces can respond to external stimuli such as light, heat, or magnetic fields, or to intrinsic stimuli associated with bacterial infection, such as a mild reduction in pH associated with the production of organic acids by bacteria or bacterial enzymes including β-lactamase or hyaluronidase,[32,33] killing bacteria on demand. For example, 660 nm light irradiation of a composite coating consisting of graphene oxide, silver nanoparticles, and collagen led to the release of antibacterial Ag^+ ions.[34] Alternating magnetic fields have been applied to induce localized heating of Ti6Al4V discs with poly(ester amide) coatings, leading to the accelerated release of rifampicin when the polymer was raised above its glass transition temperature, resulting in a synergistic heat and antibiotic-based bacterial killing.[35] Multilayered films of hyaluronic acid, chitosan, and polylysine underwent degradation in response to hyaluronidase and chymotrypsin, thereby shedding adhered bacteria and releasing antimicrobial chitosan.[36] The mild acidification associated with infection has been exploited to disrupt layered coatings composed of poly(acrylic acid) (PAA) and chitosan[37] as well as PAA and montmorillonite clay,[38] thereby releasing antibiotics. pH-change can also be harnessed to accelerate the cleavage of covalent bonds. For example, GM was immobilized by a pH-sensitive imine linkage into multilayer films composed of sodium alginate and polyethylenimine[39] and polynorbornene nanoparticles, which were subsequently attached to a titanium alloy surface.[40] Imine-conjugated GM has also been incorporated onto aldehyde-functionalized poly(glycidyl methacrylate) brushes on porous hydroxyapatite implants[41] and onto bone plate coatings composed of titanium and coated with alginate that was cross-linked with gelatin and GM.[42]

Recently, we reported the development of cationic phosphonium surfaces prepared using pH-sensitive cross-linkers that were designed to break down and release antibacterial phosphonium molecules selectively at mildly acidic pH.[43] Phosphonium coatings are attractive, as they can exhibit similar antibacterial properties compared to ammonium coatings, while providing ease of synthesis of the monomers, and higher chemical and thermal stability compared to ammoniums.[44] While our phosphonium coatings containing the more labile ketal cross-linker were quite effective in preventing bacterial colonization at pH 5, some bacteria were still observed on the surfaces. Therefore, to further enhance the efficacy of the coatings in preventing biofilm development, we report here the covalent immobilization of the antibiotic GM into the coatings by a pH-responsive imine linkage. These coatings are designed to break down and release both GM and phosphonium molecules at mildly acidic pH (Figure 1). The properties of the coatings are reported, along with the evaluation of their abilities to inhibit the formation of *S. aureus* biofilms.

EXPERIMENTAL SECTION

General Materials. Tributyl(4-vinylbenzyl)phosphonium chloride (BuP),[45] triphenyl(4-vinylbenzyl)phosphonium chloride (PhP),[45] the acetal (XA) and ketal (XK) cross-linkers[46] and 4-vinyl-

https://doi.org/10.1021/acsapm.4c02365
ACS Appl. Polym. Mater. 2024, 6, 12237−12246

benzaldehyde (VBA)[47] were prepared as previously reported. GM sulfate salt (C complex) was purchased from Toronto Research Chemicals (Toronto, Canada). H_2O_2 (30% in water), and H_2SO_4 (90−98%) were purchased from Thermo Fisher Scientific (Mississauga, Canada). Sodium acetate, acetic acid, Na_2HPO_4, NaH_2PO_4, methanol, dimethyl sulfoxide (DMSO), *N*,*N*-dimethylformamide (DMF), CH_2Cl_2, and toluene were purchased from Caledon (Halton Hills, ON, Canada). NaCl was purchased from Ambeed (Illinois, US). Fluorescamine was purchased from Sigma (St. Louis, Missouri). Ethanol (anhydrous) was purchased from Greenfield global (Brampton, ON, Canada). Triethylamine (glass distilled), 3-(trimethoxysilyl)propyl methacrylate, 2-hydroxy-2-methylpropiophenone (HMP), fluorescein sodium salt, cetyltrimethylammonium chloride solution (25 wt % in water), HCl (37%), KH_2PO_4, KCl, tryptic soy broth (TSB), agar powder, D-(+)-glucose, and chloramphenicol were purchased from Millipore Sigma (Oakville, Canada). DMSO-d_6 and D_2O were purchased from Cambridge Isotope Laboratories (Tewksbury, MA). PBS was prepared from NaCl (0.137 M), KCl (0.0027 M), Na_2HPO_4 (0.01 M), and KH_2PO_4 (0.0018 M) in distilled water, with the pH adjusted using a pH meter. Ti6Al4V (Ti) foils (Gr 5, ASTM F136, 0.05 mm thickness) were purchased from Shaanxi Yunzhong Metal Technology Co., Ltd. (Shaanxi, China).

General Methods. Infrared (IR) spectroscopy was performed using a PerkinElmer Spectrum Two FTIR spectrometer with an attenuated total reflectance (ATR) attachment and a single reflection diamond. NMR spectra were obtained in DMSO-d_6 or D_2O using a 400 MHz Bruker AvIII HD instrument. Chemical shifts were referenced to the residual solvent signals. Mass spectrometry data were obtained in positive-ion mode using a Bruker micrOTOF Waters Synapt HDSMS. Ultraviolet−visible (UV−vis) spectroscopy was performed using a Varian Cary 300 (Palo Alto, California) spectrometer at room temperature.

Synthesis of a Gentamicin-4-vinylbenzaldehyde Conjugate (GM-VBA). Gentamicin sulfate (0.2 g, 1.0 equiv, 0.42 mmol) and triethylamine (0.35 mL, 6.0 equiv, 2.5 mmol) were added to distilled water (1.5 mL). This mixture was stirred at 37 °C for 10 min to allow dissolution and then 1.5 mL of 4-vinylbenzaldehyde (1.0 equiv, 0.42 mmol) in ethanol/CH_2Cl_2 (1:1) was added. The resulting mixture was stirred for 48 h at 37 °C, resulting in precipitation of the gentamicin conjugate. The product was filtered, and then washed with distilled water followed by CH_2Cl_2 to eliminate residual starting materials. Yield = 28%. The product was a mixture of isomeric gentamicin conjugates and was characterized by ^{1}H NMR spectroscopy, IR spectroscopy, and MS (Figures 2 and S1−S4).

Substrate Preparation. Ti foils were cut into 1 cm × 1 cm squares. They were treated with piranha solution (H_2SO_4:H_2O_2, 3:1 (v/v)) for 5 min, and then incubated for 30 min in 3:1:1 H_2O:H_2O_2:HCl.[48] After thorough rinsing with deionized water and then acetone, they were dried at 50 °C in an oven for 1 h. Immediately after drying, the treated foils were immersed in 2% (v/v) 3-(trimethoxysilyl)propyl methacrylate in toluene (25 mL) overnight at room temperature, sonicated with toluene, then toluene:MeOH (1:1), and finally MeOH (5 min each). They were then dried in vacuo and used immediately.

Coating Preparation. The formulation was prepared from 43% phosphonium monomer (BuP or PhP), 50% acetal cross-linker (XA or XK), 5% HMP initiator, and 2% of GM-VBA (w/w) dissolved in DMF (∼120 μL per 30 mg of formulation). It was drop cast on treated Ti foil (20 μL of formulation per 1 cm × 1 cm square). For the determination of cross-linked content, free-standing films were prepared by wrapping the ends of untreated glass slides with tape to create a spacer, casting the film, and then placing another slide on top of the substrate. Cross-linking was achieved by passing the coating through a UV conveyor system for 5 min. The UV curing system (UV Process and Supply Inc., Illinois) was equipped with a mercury lamp with an energy and power density of UVA (1784 mJ/cm^2, 192 mW/cm^2), UVB (1647 mJ/cm^2, 178 mW/cm^2), and UVC (369 mJ/cm^2, 43 mW/cm^2), and UVV (1869 mJ/cm^2, 199 mW/cm^2) running at a speed of ∼0.06 m/s. The thickness of the coating was determined using an IP65 digital caliper. The freshly prepared coatings were washed with phosphate buffer pH 8.0 (10 mM) to remove uncross-linked material, and then rinsed with distilled water to remove salts.

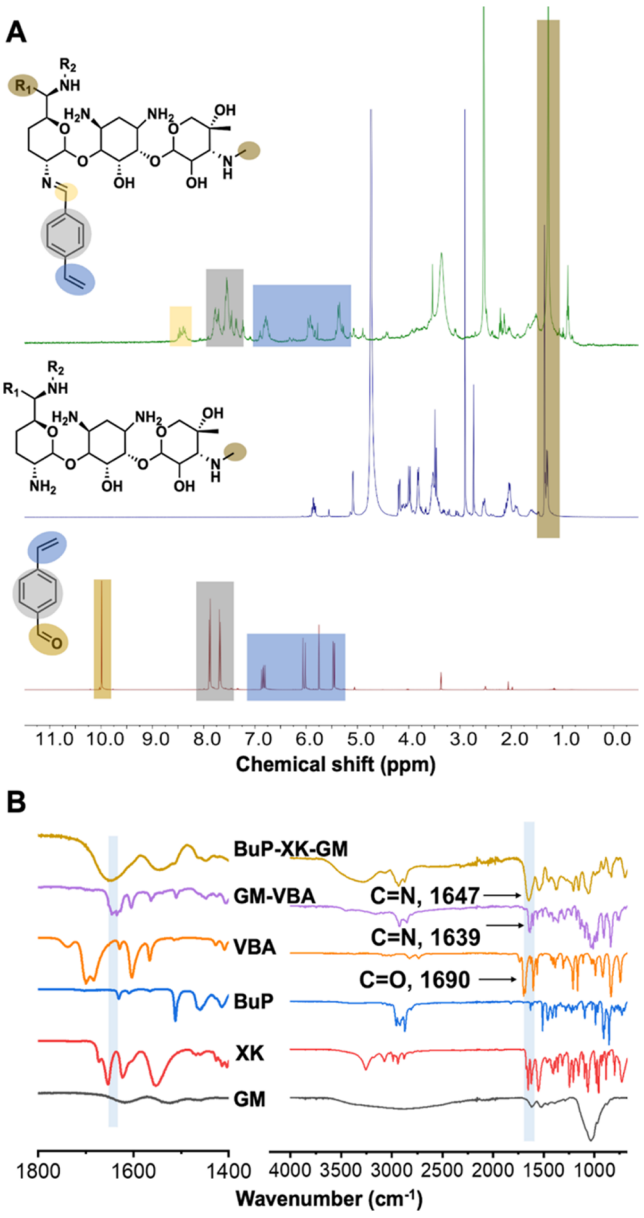

Figure 2. (A) ^{1}H NMR spectra of VBA (DMSO-d_6, 400 MHz), GM (D_2O, 400 MHz), and VBA-GM (DMSO-d_6, 400 MHz) showing the presence of signals corresponding to both GM and the aromatic and alkene groups in GM-VBA, but the disappearance of the aldehyde group and appearance of a peak at 8.5 corresponding to an imine GM-VBA. Note that the signals are broad due to the possibility for the VBA to be conjugated to the different primary amine groups on GM. (B) Overlay of the IR spectra of GM, XK, BuP, VBA, GM-VBA, and Bu-XK-GM. In the conversion of VBA to the GM-VBA conjugate, disappearance of the aldehyde stretch at ∼1700 cm^{-1} was observed, along with appearance of a peak at 1640 cm^{-1} corresponding to the imine stretch. Incorporation of GM-VBA as well as the XK cross-linker into the BuP-XK-GM coating is evidenced by the broad peak from 1600−1700 cm^{-1}. The blue box highlights the position of the imine stretch across the spectra.

Coating Properties. Cross-linked content, surface charge density, and water contact angle were measured as previously reported.[43] The full procedures are provided in the Supporting Information.

https://doi.org/10.1021/acsapm.4c02365
ACS Appl. Polym. Mater. 2024, 6, 12237−12246

GM Release from the Coatings. Coatings (1 cm^2, 50 ± 4.5 μm thickness) were each immersed in 1.5 mL of either pH 5.0, 10 mM acetate buffer or pH 7.4 PBS and incubated at 37 °C. At predetermined time points (8 h, as well as 1, 2, 3, and 4 days), the GM-containing buffer was removed and replaced with fresh buffer. The GM-containing buffer was then adjusted to pH 8.0 using 0.5 M NaOH. 75 μL of the GM-containing solution was then combined with 25 μL of fluorescamine solution (3 mg/mL in DMSO) and incubated for 15 min at room temperature in the dark. The resulting solutions were analyzed for fluorescence intensity using a Tecan Infinite M1000 Pro plate reader (Mannedorf, Switzerland) in tissue culture plates with UV transparent flat bottoms (Thermo Fisher Scientific, Mississauga, Canada). The excitation and emission wavelengths were set at 380 and 470 nm, respectively. Calibration curves were prepared using known GM standard solutions (0, 10, 20, 30, 40, and 50 μg/mL) to yield quantitative values for GM concentrations in the samples and thus the cumulative amount released. For the coatings that had fully degraded at the end of the release experiment, the total released drug from each coating was calculated to determine the GM content of the initial coating (100% release). To determine the drug loading, and thus 100% release for coatings that did not fully degrade within 4 days, 2 drops of 1 M HCl were added to facilitate complete degradation. After an additional 16 h, and once the coating had degraded, the released GM was quantified using fluorescamine as described above. The total released GM for each coating was then used to calculate the cumulative percentage of GM release at the measured time points. Each coating and condition was evaluated in triplicate and the results are presented as the mean ± standard deviation.

Bacterial Culture. *S. aureus* (ATCC 6538) was obtained from the American Type Culture Collection. Green fluorescent protein (GFP)-producing *S. aureus* (ATCC 6538) (*S. aureus*-GFP) was prepared by transformation with the plasmid pCG44 using electroporation.[49,50] The plasmid was maintained by culture of the *S. aureus* in 10 μg/mL chloramphenicol. Glycerol stocks of bacteria (1:1 bacterial suspension in TSB:50% glycerol in water) were stored at −80 °C. For an overnight bacterial culture, a scrape of glycerol stock with a sterile loop (enough to moisten the loop end) was added to 5 mL of TSB and incubated at 37 °C for 16 h under static conditions. The overnight culture was then diluted to 10^8 CFU/mL based on the optical density (OD_{600}) at λ = 600 nm (*S. aureus* OD_{600} = 0.3 ≈ 10^8 CFU/mL) for antimicrobial assays. For agar plating, tryptic soy agar was prepared by mixing 15 g of agar powder per 1 L of TSB.

Effect of Coating Degradation Products on *S. aureus*. Coated Ti foils (1 cm^2, 50 ± 4.5 μm thickness) were incubated in pH 5.0 (10 mM acetate) or pH 7.4 (10 mM phosphate) buffers (1.5 mL) for 3 days at 37 °C. Then, the pH 5.0 solutions were adjusted to pH 7.4 using 0.5 M NaOH and all solutions were passed through a 0.2 μm filter for sterilization. For the 5-fold diluted samples, 30 μL of each sterilized solution was diluted with 120 μL of sterile PBS. Then, 20 μL of each of the initial and 5-fold diluted solutions were combined with 180 μL of a 10^6 CFU/mL suspension of *S. aureus* in Mueller Hinton Broth in the wells of a 96-well plate. Four replicates of each solution were evaluated. After 16 h, bacterial viability in each well was assessed by plating 10 μL onto a tryptic soy agar plate (TSA). TSA plates were left to air-dry for 30 min before incubation at 37 °C for 16 h. The CFUs on the plates were assessed and no detectable colonies was equivalent to >99.9% inhibition based on the initial CFUs added to the solution and the 10 μL plated, while more than 50 colonies were indicated as too many to count (TMC).

Inhibition of *S. aureus* Growth on the Coatings. Coated Ti foils (1 cm^2, 50 ± 4.5 μm thickness) were sterilized by irradiation with UV light for 45 min on each side. They were then incubated in 2.5 mL of bacterial suspension (10^5 CFU/mL) in TSB supplemented with 1% glucose at 37 °C in a 24-well plate. The control samples were uncoated Ti foils treated in the same manner. Following the 16 h incubation period, bacterial viability was assessed using a drop plate method. Specifically, all coated and control samples were transferred to centrifuge tubes each containing 2 mL of PBS for the removal of the biofilms from their surfaces through vortex agitation. The resulting bacterial suspensions were diluted serially (10-fold) in sterile PBS, and then 10 μL aliquots were plated on tryptic soy agar plates. The plates were air-dried for 10 min and then incubated at 37 °C for 16 h. CFUs were subsequently counted. The control and each coating were evaluated in triplicate and the results are provided as the mean ± standard deviation. The data were analyzed using a one-way ANOVA, followed by a Tukey's posthoc test, with statistical significance established as $p < 0.05$.

Imaging of GFP-Expressing *S. aureus* on the Coatings. After overnight culture as described above, *S. aureus*-GFP was diluted to 10^7 CFU/mL in TSB with 1% glucose. Coated (1 cm^2, 50 ± 4.5 μm thickness) and uncoated control Ti foils were sterilized by UV light treatment for 45 min on each side. The coated foils were then each placed in the wells of a 24-well plate and immersed in 2.5 mL of the bacterial suspension. The samples were incubated at 37 °C for 16 h, and then gently rinsed with sterile distilled water before imaging using a Nikon Eclipse Ti2E Inverted Deconvolution Microscope (Nikon Instruments Canada Inc., Mississauga, Canada) at 20 x magnification using 465−485 nm excitation and 499−530 nm emission filters. Each coating was imaged in triplicate, with five randomly selected areas per surface images, and representative images are shown.

RESULTS AND DISCUSSION

Coating Preparation. A polymerizable imine conjugate of GM (C complex) was prepared to enable the covalent incorporation of GM into the coatings. An imine was selected because imines have been established to undergo pH-dependent hydrolysis, with more rapid cleavage at mildly acidic compared to neutral pH.[51] GM was reacted with VBA in 1:0.5:0.5 water:EtOH/CH_2Cl_2 at 37 °C, resulting in the selective precipitation of the imine conjugate (Scheme 1). The product was characterized by ^{1}H NMR spectroscopy, IR spectroscopy and mass spectrometry and determined to be a mixture of GM isomers with imine functionalization possible at different amine sites. NMR spectroscopic analysis revealed a peak at 1.26 ppm, characteristic of the $-CH_3$ groups in GM,[52] peaks from 5.8−8 ppm corresponding to the styrenic moiety, and a peak at 8.4 ppm corresponding to the CH═N− of the imine (Figure 2A).[40] The relative integrals of the signals suggested about one VBA conjugated per GM on average (Figure S3). There was no evidence of residual aldehyde from the VBA. The IR spectrum of GM-VBA had a signal at 1640 cm^{-1}, characteristic of the imine stretch,[53,54] while the absorption from the C═O stretch of the VBA at 1690 cm^{-1} disappeared (Figure 2B), which is another indication that imine formation was successful. Mass spectrometry showed masses corresponding to the conjugates of the different GM isomers (Figure S4).

The other components of the coatings, including the phosphonium monomers PhP[45] and BuP[45] as well as the cross-linkers XK[46] and XA[46] (Scheme 2) were prepared as previously reported. The formulations (Table 1) were a combination of GM-VBA (2%) with a selected phosphonium monomer (43%) and cross-linker (50%), as well as HMP as the photoinitiator (5%). The loading of GM-VBA was selected to achieve sufficiently high concentrations of released antibiotic to kill bacteria, while not compromising the integrity of the coatings. The coatings were cast on Ti foils, as this metal is commonly used in orthopedic implants. They were cured by irradiation with UV light, then washed to remove any noncovalently incorporated molecules from the cured network. Additional control coatings without GM-VBA were also prepared as previously reported.[43]

Coating Properties. The cross-linked content of the coatings after washing away noncovalently incorporated

https://doi.org/10.1021/acsapm.4c02365
ACS Appl. Polym. Mater. 2024, 6, 12237−12246

Scheme 1. Synthesis of GM-VBA from GM (C Complex, Mixture of Three Isomers)

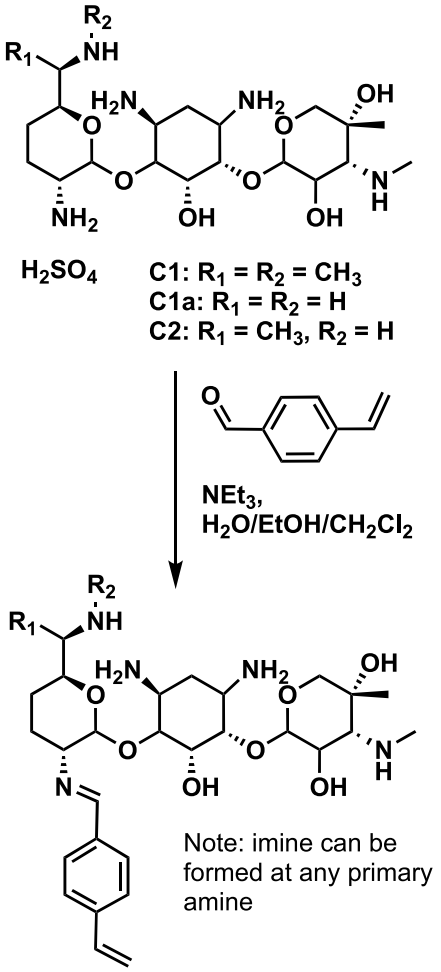

Scheme 2. Preparation of Antibacterial Coatings from GM-VBA, Phosphonium Monomer, Cross-linker, and Photoinitiator

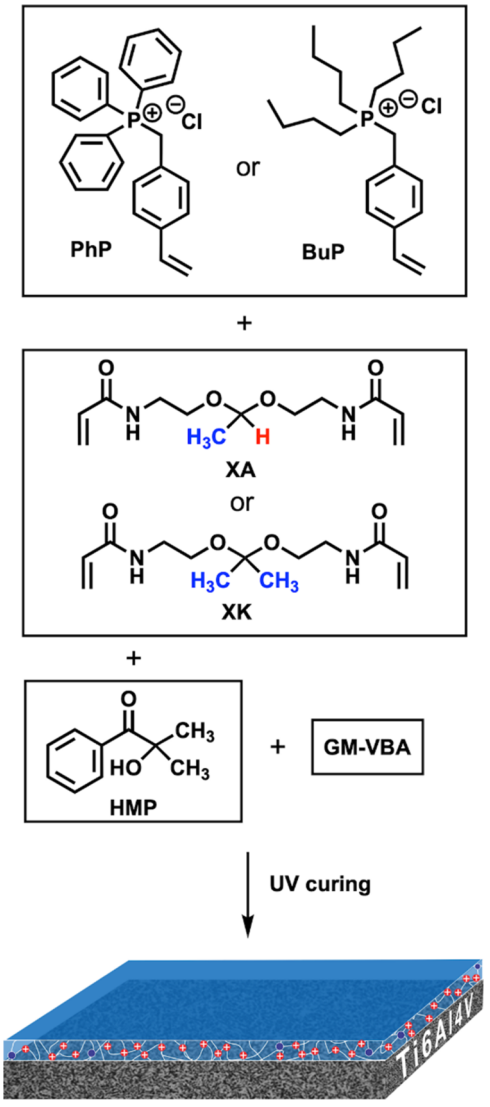

molecules was measured, and ranged from 92 to 95% for the coatings containing GM, indicating efficient cross-linking (Table 2). When the coatings with and without GM were compared, an increase in the cross-linked content for the coatings with GM was observed. This enhancement was attributed to the presence of a small percentage of GM-VBA conjugates with multiple VBAs conjugated per GM, which in principle could serve as additional cross-linkers. We evaluated the wettability of the coatings through WCA measurements. For the coatings that contained GM, WCA ranged from 29 to 45° indicating relatively hydrophilic surfaces, compared to the coatings without GM, which ranged from 51 to 62°. The hydrophilic nature of the GM coatings was attributed to the multiple hydroxyl and ammonium groups on GM. Given their crucial role in antibacterial activity, the densities of accessible cationic charges on the coating surfaces were also examined using the fluorescein dye exchange assay.[55] The cationic charge densities (c^+ = cations/cm^2) were very similar to those of the coatings without GM. They ranged from 1.7×10^{16} to 5.3×10^{16} c^+, far surpassing the minimum requirement for effective bacterial killing of exceeding 10^{14} cations/cm^2.[56] IR spectra of the coatings were also obtained and showed peaks evidencing the incorporation of the cross-linker (carbonyl stretch 1650−1700 cm^{-1}), the phosphonium monomer (2800−3000 cm^{-1}), and GM-VBA (1600−1650 cm^{-1}) (Figure 2B).

Table 1. Coating Composition in Terms of Mass Percentages of the Different Constituents

coating	GM-VBA	phosphonium monomer	cross-linker	photoinitiator (HMP)
BuP-XK-GM	2%	BuP, 43%	XK, 50%	5%
BuP-XA-GM	2%	BuP, 43%	XA, 50%	5%
PhP-XK-GM	2%	PhP, 43%	XK, 50%	5%
PhP-XA-GM	2%	PhP, 43%	XA, 50%	5%
BuP-XK	NA	BuP, 45%	XK, 50%	5%
BuP-XA	NA	BuP, 45%	XA, 50%	5%
PhP-XK	NA	PhP, 45%	XK, 50%	5%
PhP-XA	NA	PhP, 45%	XA, 50%	5%

GM Release. The pH-dependent release of GM from the coatings was investigated, as this was expected to impact their antibacterial properties. The quantification of GM in the release media was accomplished using the fluorescamine assay, which is a reliable method for measuring the concentrations of peptides, proteins, and aminoglycosides such as GM.[57,58] Fluorescamine is a nonfluorescent reagent that readily forms a

https://doi.org/10.1021/acsapm.4c02365
ACS Appl. Polym. Mater. 2024, 6, 12237−12246

Table 2. Cross-linked Content, WCA, c^+, and %GM (w/w) for the Different Coatings[a]

coating	cross-linked content (%)	WCA (deg)	c^+ (cations/cm^2)	% GM
BuP-XK-GM	92 ± 1	33 ± 2	(5.3 ± 1.3) × 10^{16}	1.8 ± 0.3
BuP-XA-GM	93 ± 1	41 ± 4	(3.3 ± 0.7) × 10^{16}	2.4 ± 0.4
PhP-XK-GM	94 ± 1	29 ± 5	(1.7 ± 0.2) × 10^{16}	2.0 ± 0.2
PhP-XA-GM	95 ± 0.3	45 ± 7	(3.4 ± 0.2) × 10^{16}	3.0 ± 0.2
BuP-XK	94 ± 2	62 ± 2	(5.9 ± 1.8) × 10^{16}	NA
BuP-XA	82 ± 0.1	59 ± 0.2	(1.8 ± 6.4) × 10^{16}	NA
PhP-XK	83 ± 2	55 ± 2	(5.6 ± 4.4) × 10^{16}	NA
PhP-XA	90 ± 2	51 ± 2	(2.2 ± 1.2) × 10^{16}	NA

[a]Values for the coatings without GM are from a previous report[43] and are included here for comparison purposes. NA = not added to the formulation.

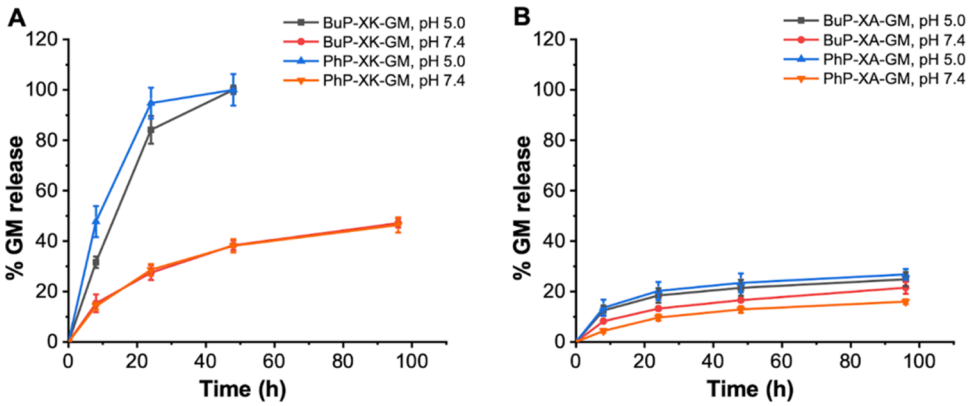

Figure 3. GM release at different pH 5.0 and 7.4 over 4 days at 37 °C: (A) GM-XK coatings; (B) GM-XA coatings.

stable, highly fluorescent product upon reaction with an amine.[59] The GM release was measured for 3 days (time period relevant to the subsequent bacterial studies) under mildly acidic conditions (pH 5.0, acetate buffer) mimicking bacterial infection[32,60] and under neutral physiological conditions (pH 7.4, PBS) at 37 °C. In each case, the GM solution was adjusted to pH 8.0 prior to fluorescamine analysis. All the coatings containing the XK cross-linker released GM more rapidly than those containing the XA cross-linker (Figure 3). For the coatings containing the XK cross-linker, the release was much faster at pH 5.0, where complete release occurred over 48 h, compared to ∼40% released at pH 7.4 over 3 days. Studies have previously reported GM release from imine linkages ranging from 20−90% at pH 5.0 and 5−10% at pH 7.4 within 8 h,[39,41,42,61] which is in general agreement with our observations for the GM-XK coatings. Previously we reported that breakdown of XA-containing phosphonium coatings occurred much more slowly than XK-containing coatings, with less than 5% degradation over 3 days, even at pH 4.5.[43] GM release for these coatings was also slower (Figure 3B), with 12−14% at pH 5.0 and 4−8% at pH 7.4 released over 3 days. Despite the acid-sensitivity of the imine linkage, it appears that coating degradation is important for GM release. It is likely that coating degradation, which involves swelling and dissolution of the coating constituents, is important for achieving water access to the imine linkage for hydrolysis. After treatment of the coatings with HCl to ensure full hydrolysis and release of GM, the loaded GM was quantified. The GM content of the coatings ranged from 1.8−3.0% (w/w), which was similar to its formulation content of 2% (w/w).

Antibacterial Activity of Coating Degradation Products on *S. aureus*. First, the coatings were assessed for their capacity to release antibacterial agents, including GM, as well as polymeric or oligomeric phosphonium molecules that could kill *S. aureus*. *S. aureus* was selected because it is the most common organism associated with periprosthetic joint infections.[62] This experiment involved incubation of the coatings in either pH 5.0 or 7.4 buffer for 3 days. After adjustment of the pH 5.0 solution to 7.4, a portion of each solution was diluted 5-fold and then the initial and diluted solutions were diluted 10-fold with *S. aureus* ATCC 6538 (10^6 CFU/mL) suspension in Mueller Hinton broth and incubated for 16 h. The resulting suspensions were plated on agar to assess bacterial viability. A finding of no CFUs indicated an antibacterial activity of >99.9% against the initial bacterial suspension (Table 3). On the other hand, more than 50 CFUs was identified as TMC, and was an indication of relatively low

Table 3. Activity of the Coating Degradation Products Released upon Incubation of the Coatings at Either pH 7.4 or 5.0[a]

	inhibition			
	pH 7.4		pH 5	
coating	initial	5 × diluted	initial	5 × diluted
BuP-XK-GM	>99.9%	TMC	>99.9%	TMC
BuP-XA-GM	TMC	TMC	TMC	TMC
PhP-XK-GM	>99.9%	TMC	>99.9%	>99.9%
PhP-XA-GM	>99.9%	TMC	>99.9%	TMC
BuP-XK	TMC	TMC	>99.9%	TMC
BuP-XA	TMC	TMC	TMC	TMC
PhP-XK	TMC	TMC	>99.9%	TMC
PhP-XA	TMC	TMC	>99.9%	TMC

[a]Both the initial solution and a 5-fold dilution were diluted 10-fold with 10^6 CFUs/mL of *S. aureus* and then drop plated on agar.

https://doi.org/10.1021/acsapm.4c02365
ACS Appl. Polym. Mater. 2024, 6, 12237−12246

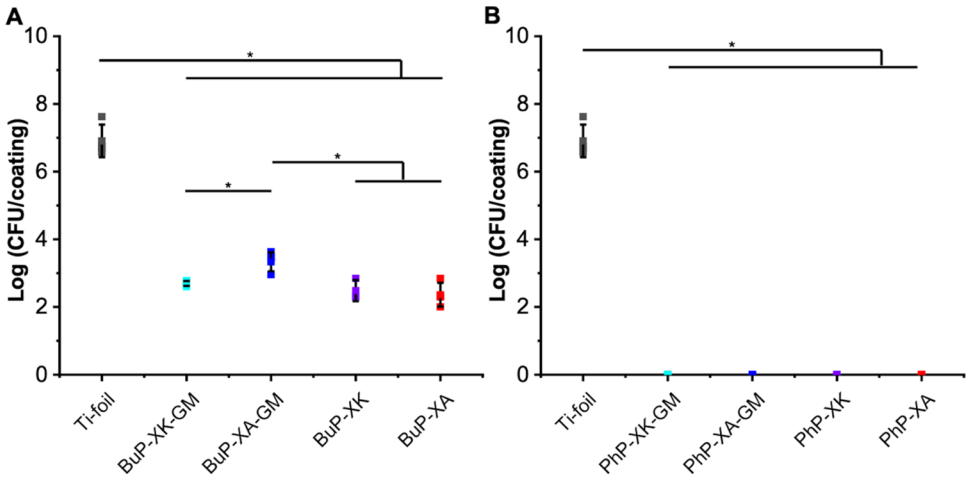

Figure 4. CFUs of *S. aureus* isolated from biofilms on different phosphonium surfaces after a 16 h incubation, determined by the drop plate method: (A) BuP coatings; (B) PhP coatings. Error bars correspond to the standard deviations ($N = 4$ surfaces). *Indicates treatments that were significantly different statistically ($p < 0.05$).

activity. The highest activity was observed for released products of the PhP-XK-GM coatings incubated at pH 5.0, for which high bacterial killing was observed for both the initial and diluted solution. The presence of GM, the more labile XK cross-linker, pH and the presence of PhP were all important for this high activity indicating the inhibition of bacterial protein synthesis by gentamicin as well as membrane disruption by the phosphonium species were both likely involved in the mechanism of bacterial inhibition. Changing the pH to 7.4 for PhP-XK-GM reduced activity such that only the initial solution was highly active, while changing to the more slowly hydrolyzing cross-linker XA had the same effect. Either of these changes would reduce the levels of antibacterial molecules released into solution. The PhP-XK coating without GM was also less active, indicating the important role of the antibiotic. Overall, the activities of the molecules released from the BuP coatings were consistently lower than for the corresponding PhP coatings. These results are in agreement with our own recent results for coatings based on PhP and BuP,[43] as well as previous studies by Kanazawa et al. showing higher activity of PhP polymers compared to BuP polymers against *S. aureus*.[63] However, BuP-XK did show activity of the initial solution from incubation at pH 5, indicating sufficient phosphonium release under these conditions, while the initial solutions from the BuP-XK-GM coatings showed activity at both pH 7.4 and 5.0, indicating that sufficient antibiotic release can occur to provide some activity at pH 7.4. Released products from the BuP-XA and BuP-XA-GM coatings were inactive, consistent with the expected low levels of release of both phosphonium[43] and antibiotic (Figure 3).

Inhibition of *S. aureus* Growth on the Coatings. Next, the coatings were evaluated for their ability to inhibit the growth of *S. aureus* in direct contact with their surfaces. Using crystal violet for biofilm quantification was explored initially, but this reagent bound to the coatings themselves, so quantitative assessment could not be performed. Therefore, we evaluated bacterial CFUs isolated from the coatings. The coatings were exposed to a 10^5 CFU/mL suspension of *S. aureus* (ATCC 6538) in TSB (pH 7.4) supplemented with 1% glucose. After a 16 h incubation at 37 °C, the bacteria were detached by vortexing the biofilms, then the resulting suspensions were serially diluted and plated on agar for counting. All PhP-based coatings completely inhibited the growth of bacteria on the surfaces, irrespective of GM incorporation, while the BuP coatings led to a ∼ 4 log reduction in bacteria (Figure 4). The higher activity of the PhP coatings is consistent with the results described above (Table 3). Among the BuP coatings, BuP-XK-GM, BuP-XK, and BuP-XA were slightly more effective in reducing bacteria on the surface compared to BuP-XA-GM. It is not clear why BuP-XA-GM would be less active than the analogous coating without GM, but the dominant role of direct surface-mediated bacterial killing activity via phosphonium-mediated membrane disruption in this experiment may explain the lack of added activity from the antibiotic.

The high antibacterial activity of all the coatings, even without antibiotics, was initially surprising considering our recent results[43] where substantial *S. aureus* growth was observed on PhP-XA and BuP-XA coatings, even in pH 5.0 buffer. However, there are important differences between the two experiments. First, the previous experiments were performed in simple pH 7.4 and pH 5 buffers, while the current experiments were performed in TSB supplemented with 1% glucose. In addition, due to the higher proliferation of *S. aureus* and ease of biofilm formation in this medium, only 10^5 CFU/mL were used, compared to 10^7 in the previous study in simple buffers. While the TSB medium promotes bacterial proliferation, the lower initial bacterial loading in the present study may have played a role in enhancing the coating efficacy. In addition, antimicrobial agents may be more effective against the actively dividing cells.[64] It should also be noted that while the initial pH of the TSB was 7.4, its buffer concentration is only 14 mM, and the rapid growth of bacteria in this medium was observed to acidify the solution to ∼pH 5, thereby activating the coating in a manner similar to the experiments performed at pH 5. In any case, the high activities of the surfaces are in line with those of other cationic surfaces with similar cationic charge densities,[43−45] indicating that with high surface killing activity it may be difficult to observe the effect of the antibiotic.

Fluorescence microscopy of GFP-*S. aureus* on the phosphonium coatings was performed after incubation of the coatings with 10^7 CFU/mL of bacteria in TSB with 1% glucose for 16 h. In agreement with the CFU quantification presented

https://doi.org/10.1021/acsapm.4c02365
ACS Appl. Polym. Mater. 2024, 6, 12237−12246

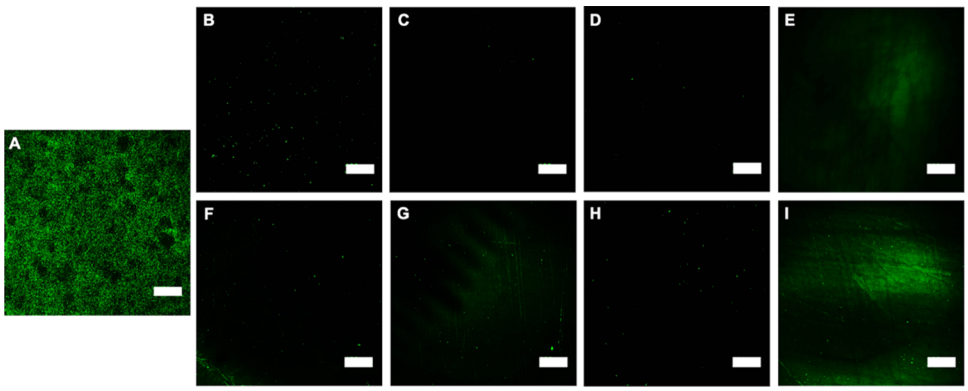

Figure 5. Fluorescence microscopy images of *S. aureus-GFP* adhered to GM coatings after 16 h incubation at 10^7 CFU/mL. (A) Uncoated Ti substrate, (B) BuP-XK-GM, (C) BuP-XA-GM, (D) BuP-XK, (E) BuP-XA, (F) PhP-XK-GM, (G) PhP-XA-GM, (H) PhP-XK, and (I) PhP-XA. Representative images are shown. Scale bar = 100 μm.

in Figure 4, high levels of GFP-*S. aureus* were observed on the control surface, whereas only trace levels were observed on any of the coatings (Figure 5), even with the challenge of 10^7 CFUs/mL. Unfortunately, quantification of surface-adhered bacteria proved impossible due to the autofluorescence exhibited by the coating itself (e.g., Figure 5E,I).

CONCLUSIONS

A pH-sensitive GM-VBA conjugate containing an imine linkage was successfully synthesized and then copolymerized into cationic phosphonium coatings containing BuP or PhP monomers and XA or XK cross-linkers. Each coating exhibited high cross-linked content of >92%, and at least 10^{16} accessible cations/cm^2. XK coatings released 100% of GM within 2 days at pH 5.0, whereas at pH 7.4, the release was limited to less than 30%. In contrast, XA coatings exhibited GM release between 15−20% under either condition over 2 days at both pH values. The efficacy of these coatings against *S. aureus* was evaluated through exposure of the coating degradation products to planktonic bacteria and through direct contact of bacteria with the coatings through CFU counting and imaging of GFP-*S. aureus* on the surfaces. Studies of the coating degradation products indicated that the products from the PhP-XK-GM coatings were the most active, while removing the GM, changing to the XA cross-linker, or changing to BuP led to lower activity. In the direct contact studies, all PhP-based coatings, regardless of GM incorporation, were highly active, with a ∼7 log reduction of CFUs compared to control surfaces. The high activity levels, even in the absence of GM or high degradability, indicated the dominant role of surface contact killing by membrane disruption in these experiments. BuP-based coatings also presented high levels of activity (∼4 log reduction), and did not show a dependence on antibiotic or cross-linker, again indicating that the coatings could kill by contact. Fluorescence microscopy analysis indicated that only trace levels of bacteria could be observed on the surfaces, even when exposed to 10^7 CFUs/mL of GFP-*S. aureus*. Overall, these results indicate the high efficacy of these coatings in killing bacteria. The more stable coatings containing the XA cross-linker may be beneficial in preventing colonization of the bacteria on surfaces such as those used in hospitals, food preparation, or water treatment, while releasing minimal levels of antibiotic and phosphonium into the surrounding environment. On the other hand, in addition to its high surface activity, PhP-XK-GM shows the greatest potential to release biocidal molecules for the killing of bacteria in the surrounding environment of the surface, making it of potential interest for medical device coatings, provided that a suitable balance between the antibacterial activity and toxicity of the released phosphonium species can be achieved. The approach for antibiotic immobilization into these coatings should also be generalizable to other important aminoglycoside antibiotics such as netilmicin, amikacin, neomycin, and tobramycin, which can be investigated in future research.

ASSOCIATED CONTENT

Supporting Information

The Supporting Information is available free of charge at https://pubs.acs.org/doi/10.1021/acsapm.4c02365.

Additional experimental procedures for coating characterization, NMR spectra and mass spectrometry data for the GM-VBA conjugate (PDF)

AUTHOR INFORMATION

Corresponding Author

Elizabeth R. Gillies − *School of Biomedical Engineering, The University of Western Ontario, London, Ontario, Canada N6A 5B9; Department of Chemistry, The University of Western Ontario, London, Ontario, Canada N6A 5B7; Department of Chemical and Biochemical Engineering, The University of Western Ontario, London, Ontario, Canada N6A 5B9;* orcid.org/0000-0002-3983-2248; Email: egillie@uwo.ca

Authors

Mónica Vásquez Peña − *School of Biomedical Engineering, The University of Western Ontario, London, Ontario, Canada N6A 5B9*

Paul J. Ragogna − *Department of Chemistry, The University of Western Ontario, London, Ontario, Canada N6A 5B7; Surface Science Western, London, Ontario, Canada N6G 0J3;* orcid.org/0000-0003-2727-7635

Complete contact information is available at: https://pubs.acs.org/10.1021/acsapm.4c02365

Notes

The authors declare no competing financial interest.

■ ACKNOWLEDGMENTS

We thank the Natural Sciences and Engineering Research Council of Canada (RGPIN-2021-04377 to P.J.R. and RGPIN-2021-03950 to E.R.G.); the Canada Research Chair program (CRC-2020-00101 for E.R.G.), and CONACYT (Mexico, fellowship for M.V.P.) for funding. We thank Syensqo for supplying organophosphines, the Heinrichs laboratory for the GFP-expressing bacteria, and the Biotron Integrated Microscopy Facility for assistance with fluorescence microscopy.

■ REFERENCES

(1) Galié, S.; García-Gutiérrez, C.; Miguélez, E. M.; Villar, C. J.; Lombó, F. Biofilms in the Food Industry: Health Aspects and Control Methods. *Front. Microbiol.* **2018**, *9*, No. 898.
(2) Francolini, I.; Hall-Stoodley, L.; Stoodley, P. Biofilms, Biomaterials, and Device-Related Infections. In *Biomaterials Science*; Elsevier, 2020; pp 823−840.
(3) Kamath, A. F.; Ong, K. L.; Lau, E.; Chan, V.; Vail, T. P.; Rubash, H. E.; Berry, D. J.; Bozic, K. J. Quantifying the Burden of Revision Total Joint Arthroplasty for Periprosthetic Infection. *J. Arthroplasty* **2015**, *30* (9), 1492−1497.
(4) Moriarty, T. F.; Kuehl, R.; Coenye, T.; Metsemakers, W. J.; Morgenstern, M.; Schwarz, E. M.; Riool, M.; Zaat, S. A. J.; Khana, N.; Kates, S. L.; Richards, R. G. Orthopaedic Device-Related Infection: Current and Future Interventions for Improved Prevention and Treatment. *EFORT Open Rev.* **2016**, *1* (4), 89−99.
(5) Kranjec, C.; Morales Angeles, D.; Torrissen Mårli, M.; Fernández, L.; García, P.; Kjos, M.; Diep, D. B. Staphylococcal Biofilms: Challenges and Novel Therapeutic Perspectives. *Antibiotics* **2021**, *10* (2), 131.
(6) Yin, R.; Cheng, J.; Wang, J.; Li, P.; Lin, J. Treatment of *Pseudomonas Aeruginosa* Infectious Biofilms: Challenges and Strategies. *Front. Microbiol.* **2022**, *13*, No. 955286.
(7) Mirza, Y. H.; Tansey, R.; Sukeik, M.; Shaath, M.; Haddad, F. S. Biofilm and the Role of Antibiotics in the Treatment of Periprosthetic Hip and Knee Joint Infections. *Open Orthop. J.* **2016**, *10* (Suppl-2, M6), 636.
(8) Le Vavasseur, B.; Zeller, V. Antibiotic Therapy for Prosthetic Joint Infections: An Overview. *Antibiotics* **2022**, *11* (4), 486.
(9) Darouiche, R. O. Treatment of Infections Associated with Surgical Implants. *N. Engl. J. Med.* **2004**, *350* (14), 1422−1429.
(10) Charette, R. S.; Melnic, C. M. Two-Stage Revision Arthroplasty for the Treatment of Prosthetic Joint Infection. *Curr. Rev. Musculoskelet. Med.* **2018**, *11* (3), 332−340.
(11) Slane, J.; Gietman, B.; Squire, M. Antibiotic Elution from Acrylic Bone Cement Loaded with High Doses of Tobramycin and Vancomycin. *J. Orthop. Res.* **2018**, *36* (4), 1078−1085.
(12) Hinarejos, P.; Guirro, P.; Puig-Verdie, L.; Torres-Claramunt, R.; Leal-Blanquet, J.; Sanchez-Soler, J.; Monllau, J. C. Use of Antibiotic-Loaded Cement in Total Knee Arthroplasty. *World J. Orthop.* **2015**, *6* (11), 877.
(13) van de Belt, H.; Neut, D.; Schenk, W.; van Horn, J. R.; van der Mei, H. C.; Busscher, H. J. *Staphylococcus Aureus* Biofilm Formation on Different Gentamicin-Loaded Polymethylmethacrylate Bone Cements. *Biomaterials* **2001**, *22* (12), 1607−1611.
(14) Ene, R.; Nica, M.; Ene, D.; Cursaru, A.; Cirstoiu, C. Review of Calcium-Sulphate-Based Ceramics and Synthetic Bone Substitutes Used for Antibiotic Delivery in PJI and Osteomyelitis Treatment. *EFORT Open Rev.* **2021**, *6* (5), 297−304.
(15) McConoughey, S. J.; Howlin, R. P.; Wiseman, J.; Stoodley, P.; Calhoun, J. H. Comparing PMMA and Calcium Sulfate as Carriers for the Local Delivery of Antibiotics to Infected Surgical Sites. *J. Biomed. Mater. Res., Part B* **2015**, *103* (4), 870−877.
(16) Laycock, P. A.; Cooper, J. J.; Howlin, R. P.; Delury, C.; Aiken, S.; Stoodley, P. In Vitro Efficacy of Antibiotics Released from Calcium Sulfate Bone Void Filler Beads. *Materials* **2018**, *11* (11), 2265.
(17) Dusane, D. H.; Diamond, S. M.; Knecht, C. S.; Farrar, N. R.; Peters, C. W.; Howlin, R. P.; Swearingen, M. C.; Calhoun, J. H.; Plaut, R. D.; Nocera, T. M.; Granger, J. F.; Stoodley, P. Effects of Loading Concentration, Blood and Synovial Fluid on Antibiotic Release and Anti-Biofilm Activity of Bone Cement Beads. *J. Controlled Release* **2017**, *248*, 24−32.
(18) Chen, C.-P.; Wickstrom, E. Self-Protecting Bactericidal Titanium Alloy Surface Formed by Covalent Bonding of Daptomycin Bisphosphonates. *Bioconjugate Chem.* **2010**, *21* (11), 1978−1986.
(19) Jose, B.; Antoci, V.; Zeiger, A. R.; Wickstrom, E.; Hickok, N. J. Vancomycin Covalently Bonded to Titanium Beads Kills Staphylococcus Aureus. *Chem. Biol.* **2005**, *12* (9), 1041−1048.
(20) Bonilla-Gameros, L.; Chevallier, P.; Sarkissian, A.; Mantovani, D. Silver-Based Antibacterial Strategies for Healthcare-Associated Infections: Processes, Challenges, and Regulations. An Integrated Review. *Nanomedicine* **2020**, *24*, No. 102142.
(21) Chug, M. K.; Brisbois, E. J. Recent Developments in Multifunctional Antimicrobial Surfaces and Applications toward Advanced Nitric Oxide-Based Biomaterials. *ACS Mater. Au* **2022**, *2* (5), 525−551.
(22) Wang, Y.; Wang, F.; Zhang, H.; Yu, B.; Cong, H.; Shen, Y. Antibacterial Material Surfaces/Interfaces for Biomedical Applications. *Appl. Mater. Today* **2021**, *25*, No. 101192.
(23) Si, Z.; Zheng, W.; Prananty, D.; Li, J.; Koh, C. H.; Kang, E.-T.; Pethe, K.; Chan-Park, M. B. Polymers as Advanced Antibacterial and Antibiofilm Agents for Direct and Combination Therapies. *Chem. Sci.* **2022**, *13* (2), 345−364.
(24) Cuthbert, T. J.; Harrison, T. D.; Ragogna, P. J.; Gillies, E. R. Synthesis, Properties, and Antibacterial Activity of Polyphosphonium Semi-Interpenetrating Networks. *J. Mater. Chem. B* **2016**, *4* (28), 4872−4883.
(25) Xu, X.; Wang, Q.; Chang, Y.; Zhang, Y.; Peng, H.; Whittaker, A. K.; Fu, C. Antifouling and Antibacterial Surfaces Grafted with Sulfur-Containing Copolymers. *ACS Appl. Mater. Interfaces* **2022**, *14* (36), 41400−41411.
(26) Chen, P.; Lang, J.; Zhou, Y.; Khlyustova, A.; Zhang, Z.; Ma, X.; Liu, S.; Cheng, Y.; Yang, R. An Imidazolium-Based Zwitterionic Polymer for Antiviral and Antibacterial Dual Functional Coatings. *Sci. Adv.* **2022**, *8* (2), No. eabl8812.
(27) Yu, Q.; Zhang, Y.; Wang, H.; Brash, J.; Chen, H. Anti-Fouling Bioactive Surfaces. *Acta Biomater.* **2011**, *7* (4), 1550−1557.
(28) Gevrek, T. N.; Yu, K.; Kizhakkedathu, J. N.; Sanyal, A. Thiol-Reactive Polymers for Titanium Interfaces: Fabrication of Antimicrobial Coatings. *ACS Appl. Polym. Mater.* **2019**, *1* (6), 1308−1316.
(29) Wei, T.; Yu, Q.; Chen, H. Responsive and Synergistic Antibacterial Coatings: Fighting Against Bacteria in a Smart and Effective Way. *Adv. Healthcare Mater.* **2019**, *8* (3), No. 1801381.
(30) Li, X.; Wu, B.; Chen, H.; Nan, K.; Jin, Y.; Sun, L.; Wang, B. Recent Developments in Smart Antibacterial Surfaces to Inhibit Biofilm Formation and Bacterial Infections. *J. Mater. Chem. B* **2018**, *6* (26), 4274−4292.
(31) Wei, T.; Qu, Y.; Zou, Y.; Zhang, Y.; Yu, Q. Exploration of Smart Antibacterial Coatings for Practical Applications. *Curr. Opin. Chem. Eng.* **2021**, *34*, No. 100727.
(32) Bjarnsholt, T.; Whiteley, M.; Rumbaugh, K. P.; Stewart, P. S.; Jensen, PØ.; Frimodt-Møller, N. The Importance of Understanding the Infectious Microenvironment. *Lancet Infect. Dis.* **2022**, *22* (3), e88−e92.
(33) Smith, S. M. D-Lactic Acid Production as a Monitor of the Effectiveness of Antimicrobial Agents. *Antimicrob. Agents Chemother.* **1991**, *35* (2), 237−241.
(34) Xie, X.; Mao, C.; Liu, X.; Zhang, Y.; Cui, Z.; Yang, X.; Yeung, K. W.; Pan, H.; Chu, P. K.; Wu, S. Synergistic Bacteria Killing through Photodynamic and Physical Actions of Graphene Oxide/Ag/Collagen Coating. *ACS Appl. Mater. Interfaces* **2017**, *9* (31), 26417−26428.
(35) Kwan, J. C.; Flannagan, R. S.; Vásquez Peña, M.; Heinrichs, D. E.; Holdsworth, D. W.; Gillies, E. R. Induction Heating Triggers Antibiotic Release and Synergistic Bacterial Killing on Polymer-

Coated Titanium Surfaces. *Adv. Healthcare Mater.* **2023**, *12* (22), No. 2202807.
(36) Yao, Q.; Ye, Z.; Sun, L.; Jin, Y.; Xu, Q.; Yang, M.; Wang, Y.; Zhou, Y.; Ji, J.; Chen, H.; Wang, B. Bacterial Infection Microenvironment-Responsive Enzymatically Degradable Multilayer Films for Multifunctional Antibacterial Properties. *J. Mater. Chem. B* **2017**, *5* (43), 8532−8541.
(37) Nalam, P. C.; Lee, H.-S.; Bhatt, N.; Carpick, R. W.; Eckmann, D. M.; Composto, R. J. Nanomechanics of pH-Responsive, Drug-Loaded, Bilayered Polymer Grafts. *ACS Appl. Mater. Interfaces* **2017**, *9* (15), 12936−12948.
(38) Pavlukhina, S.; Zhuk, I.; Mentbayeva, A.; Rautenberg, E.; Chang, W.; Yu, X.; Van De Belt-gritter, B.; Busscher, H. J.; Van der Mei, H. C.; Sukhishvili, S. A. Small-Molecule-Hosting Nanocomposite Films with Multiple Bacteria-Triggered Responses. *NPG Asia Mater.* **2014**, *6* (8), No. e121.
(39) Li, M.; Wang, H.; Chen, X.; Jin, S.; Chen, W.; Meng, Y.; Liu, Y.; Guo, Y.; Jiang, W.; Xu, X.; Wang, B. Chemical Grafting of Antibiotics into Multilayer Films through Schiff Base Reaction for Self-Defensive Response to Bacterial Infections. *Chem. Eng. J.* **2020**, *382*, No. 122973.
(40) Pichavant, L.; Amador, G.; Jacqueline, C.; Brouillaud, B.; Héroguez, V.; Durrieu, M.-C. pH-Controlled Delivery of Gentamicin Sulfate from Orthopedic Devices Preventing Nosocomial Infections. *J. Controlled Release* **2012**, *162* (2), 373−381.
(41) Jin, X.; Xiong, Y. H.; Zhang, X. Y.; Wang, R.; Xing, Y.; Duan, S.; Chen, D.; Tian, W.; Xu, F. J. Self-Adaptive Antibacterial Porous Implants with Sustainable Responses for Infected Bone Defect Therapy. *Adv. Funct. Mater.* **2019**, *29* (17), No. 1807915.
(42) Zhang, L.; Yang, Y.; Xiong, Y.-H.; Zhao, Y.-Q.; Xiu, Z.; Ren, H.-M.; Zhang, K.; Duan, S.; Chen, Y.; Xu, F.-J. Infection-Responsive Long-Term Antibacterial Bone Plates for Open Fracture Therapy. *Bioact. Mater.* **2023**, *25*, 1−12.
(43) Vásquez Peña, M.; Nygard, K.; Ragogna, P. J.; Gillies, E. R. pH-Responsive Antibacterial Surfaces Based on Cross-Linked Phosphonium Polymers. *ACS Appl. Polym. Mater.* **2024**, *6* (11), 6208−6218.
(44) Bradaric, C. J.; Downard, A.; Kennedy, C.; Robertson, A. J.; Zhou, Y. Industrial Preparation of Phosphonium Ionic Liquids. *Green Chem.* **2003**, *5* (2), 143−152.
(45) Harrison, T. D.; Ragogna, P. J.; Gillies, E. R. Phosphonium Hydrogels for Controlled Release of Ionic Cargo. *Chem. Commun.* **2018**, *54* (79), 11164−11167.
(46) Jain, R.; Standley, S. M.; Frechet, J. M. Synthesis and Degradation of pH-Sensitive Linear Poly(amidoamine)s. *Macromolecules* **2007**, *40* (3), 452−457.
(47) Jackson, A. W.; Stakes, C.; Fulton, D. A. The Formation of Core Cross-Linked Star Polymer and Nanogel Assemblies Facilitated by the Formation of Dynamic Covalent Imine Bonds. *Polym. Chem.* **2011**, *2* (11), 2500−2511.
(48) Hasan, A.; Saxena, V.; Pandey, L. M. Surface Functionalization of Ti6Al4V Via Self-Assembled Monolayers for Improved Protein Adsorption and Fibroblast Adhesion. *Langmuir* **2018**, *34* (11), 3494−3506.
(49) Gries, C. M.; Sadykov, M. R.; Bulock, L. L.; Chaudhari, S. S.; Thomas, V. C.; Bose, J. L.; Bayles, K. W. Potassium Uptake Modulates Staphylococcus Aureus Metabolism. *Msphere* **2016**, *1* (3), No. e00125-16.
(50) Flannagan, R. S.; Heinrichs, D. E. A Fluorescence Based-Proliferation Assay for the Identification of Replicating Bacteria within Host Cells. *Front. Microbiol.* **2018**, *9*, No. 3084.
(51) Cordes, E. H.; Jencks, W. On the Mechanism of Schiff Base Formation and Hydrolysis. *J. Am. Chem. Soc.* **1962**, *84* (5), 832−837.
(52) Deubner, R.; Schollmayer, C.; Wienen, F.; Holzgrabe, U. Assignment of the Major and Minor Components of Gentamicin for Evaluation of Batches. *Magn. Reson. Chem.* **2003**, *41* (8), 589−598.
(53) Hoque, J.; Bhattacharjee, B.; Prakash, R. G.; Paramanandham, K.; Haldar, J. Dual Function Injectable Hydrogel for Controlled Release of Antibiotic and Local Antibacterial Therapy. *Biomacromolecules* **2018**, *19* (2), 267−278.
(54) Nguyen, T.-K.; Selvanayagam, R.; Ho, K. K.; Chen, R.; Kutty, S. K.; Rice, S. A.; Kumar, N.; Barraud, N.; Duong, H. T.; Boyer, C. Co-Delivery of Nitric Oxide and Antibiotic Using Polymeric Nanoparticles. *Chem. Sci.* **2016**, *7* (2), 1016−1027.
(55) Murata, H.; Koepsel, R. R.; Matyjaszewski, K.; Russell, A. J. Permanent, Non-Leaching Antibacterial Surfaces—2: How High Density Cationic Surfaces Kill Bacterial Cells. *Biomaterials* **2007**, *28* (32), 4870−4879.
(56) Kügler, R.; Bouloussa, O.; Rondelez, F. Evidence of a Charge-Density Threshold for Optimum Efficiency of Biocidal Cationic Surfaces. *Microbiology* **2005**, *151* (5), 1341−1348.
(57) Tekkeli, S. E. K.; Önal, A.; Sağırlı, A. O. Spectrofluorimetric Determination of Tobramycin in Human Serum and Pharmaceutical Preparations by Derivatization with Fluorescamine. *Luminescence* **2014**, *29* (1), 87−91.
(58) Chen, A. C.; Mayer, R. T. Fluorescamine as a Tool for Amino Sugar Analysis. *J. Chromatogr. A* **1981**, *207* (3), 445−448.
(59) Udenfriend, S.; Stein, S.; Boehlen, P.; Dairman, W.; Leimgruber, W.; Weigele, M. Fluorescamine: A Reagent for Assay of Amino Acids, Peptides, Proteins, and Primary Amines in the Picomole Range. *Science* **1972**, *178* (4063), 871−872.
(60) Wang, X.; Shan, M.; Zhang, S.; Chen, X.; Liu, W.; Chen, J.; Liu, X. Stimuli-Responsive Antibacterial Materials: Molecular Structures, Design Principles, and Biomedical Applications. *Adv. Sci.* **2022**, *9* (13), No. 2104843.
(61) Xiang, Y.; Jin, R.; Zhang, Y.; Li, K.; Liu, G.; Song, X.; Wang, Y.; Nie, Y. Foldable Glistening-Free Acrylic Intraocular Lens Biomaterials with Dual-Side Heterogeneous Surface Modification for Postoperative Endophthalmitis and Posterior Capsule Opacification Prophylaxis. *Biomacromolecules* **2021**, *22* (8), 3510−3521.
(62) Baratz, M. D.; Hallmark, R.; Odum, S. M.; Springer, B. D. Twenty Percent of Patients May Remain Colonized with Methicillin-Resistant Staphylococcus Aureus Despite a Decolonization Protocol in Patients Undergoing Elective Total Joint Arthroplasty. *Clin. Orthop. Relat. Res.* **2015**, *473*, 2283−2290.
(63) Kanazawa, A.; Ikeda, T.; Endo, T. Novel Polycationic Biocides: Synthesis and Antibacterial Activity of Polymeric Phosphonium Salts. *J. Polym. Sci., Part A: Polym. Chem.* **1993**, *31* (2), 335−343.
(64) Ocampo, P. S.; Lázár, V.; Papp, B.; Arnoldini, M.; Abel zur Wiesch, P.; Busa-Fekete, R.; Fekete, G.; Pál, C.; Ackermann, M.; Bonhoeffer, S. Antagonism between Bacteriostatic and Bactericidal Antibiotics Is Prevalent. *Antimicrob. Agents Chemother.* **2014**, *58* (8), 4573−4582.

https://doi.org/10.1021/acsapm.4c02365
ACS Appl. Polym. Mater. 2024, 6, 12237−12246